

## Response to Anonymous Referee #1

We appreciate the comprehensive, practical, and instructive comments of referee #1. They have helped us improving the paper. We are responding to the comments in the following way:

*- The data are presented but the calibration system is not well described and it is questionable to know if it is adapted to the Neumayer conditions. It would be nice to display the calibration curves obtained to correct for the instrumental drift (down to 100 ppm according to the text) as well as the influence of humidity on water isotopic ratio in the humidity range studied here. A section dedicated to calibration should be added in the supplementary material.*

We added a subsection called “Calibration program for water vapour isotope measurements” in the supplementary (revised manuscript, Appendix A). Here, we explain all parts of the calibration program and show the humidity response curves:

Revised manuscript, Appendix A, line 582:

Appendix A: Calibration program for water vapour isotope measurements

To apply the calibration, we defined a calibration protocol modifying the protocol developed by Steen-Larsen et al. (2013) and Bonne et al. (2014). Based on the protocol we need to correct the isotopic observation in four aspects: the humidity concentration dependence of isotopic measurements, the potential long-term drift of the instrument, the offset between measured and real isotope values, and the wrong measurements related to special events.

To calibrate the instrument, we need to measure different known water stable isotopes in different conditions. One of the modifications of the initial protocol is related to the method of producing water vapour for the calibration. We consider 4 glass bottles (named "bubbler" with a number from 1 to 4) of water standards with known isotopic compositions, kept at a constant temperature. The water vapour with adjustable humidity is made by blowing dry air into the bubblers and making bubbles. For Picarro L2140-i the range of water concentration is originally defined between 1000 and 50000 ppm. For humidity values below 2000 ppm, systematic instrumental errors in the measured isotope values need to be corrected by so-called humidity response functions (see Steen-Larsen et al., 2014b, for details). In order to determine the humidity response functions of our calibration setup, we measure different known isotopic compositions over a range of water concentrations between 100 and 10000 ppm and computed the humidity response functions as the interpolation of the distribution of all measurements for each standard, using a polynomial function of 2nd order (Fig. A1). Humidity response sequences are measured once per year and for this study the humidity response functions of two years (January 2018 and January 2019) have been considered. The calibration system at Neumayer Station was also modified based on the isotopic composition of water vapour at Neumayer Station and used 3 different isotopic water standards (liquid), with  $\delta^{18}\text{O}$  values of  $-6.07\pm 0.1\text{‰}$  (around  $-17\text{‰}$  in water vapour),  $-25.33\pm 0.1\text{‰}$  (around  $-36\text{‰}$  in water vapour), and

-43.80±0.1 ‰ (around -54 ‰ in water vapour).  $\delta D$  values of the standards (water liquid) are -43.73±1.5‰, -195.21±1.5‰, and -344.57±1.5‰. One of the isotope standards ( $\delta^{18}O = -25.33‰$ ) is used for quality control in not one but two of the four bubblers. Every year in January, a sample of each standard is taken and transferred to a laboratory in AWI Bremerhaven and was measured in order to know the isotopic composition. In this study, no change in the isotopic compositions of the standards has been detected. Water standards with water vapour  $\delta^{18}O$  values of around -54‰, -36‰, and -17‰, cover the whole isotopic measurements range in water vapour at Neumayer Station. The correction of humidity dependant water vapour isotopic measurements has been done by a linear interpolation of those two moisture response functions that belong to the isotopic standards above and below each measured isotopic value. After applying the humidity response calibration, the correction of the measurements based on the instrumental drift and offset is done. We measure the isotopic composition of all water standards every 25 hours. Such 25-hour cycle avoids repetition of the daily calibration at the same time every day but moves the calibration time 1 hour forward per day. By such a calibration interval, we avoid missing the same time period during all days in all measurements. Each isotopic standard is measured for 30 minutes, and to avoid any memory effects, we consider the mean value of the last 15 minutes of each measured water standard, only. If the calibration measurements are not stable enough, we filter them. To correct the data based on the instrumental drift, we consider the average of 14 days of measurements, 7 days before and 7 days after the day that we want to correct its data. The correction of the instrumental drift and offset are done by a linear interpolation of the two closest mean isotopic standards, measured at the 25-hour interval.

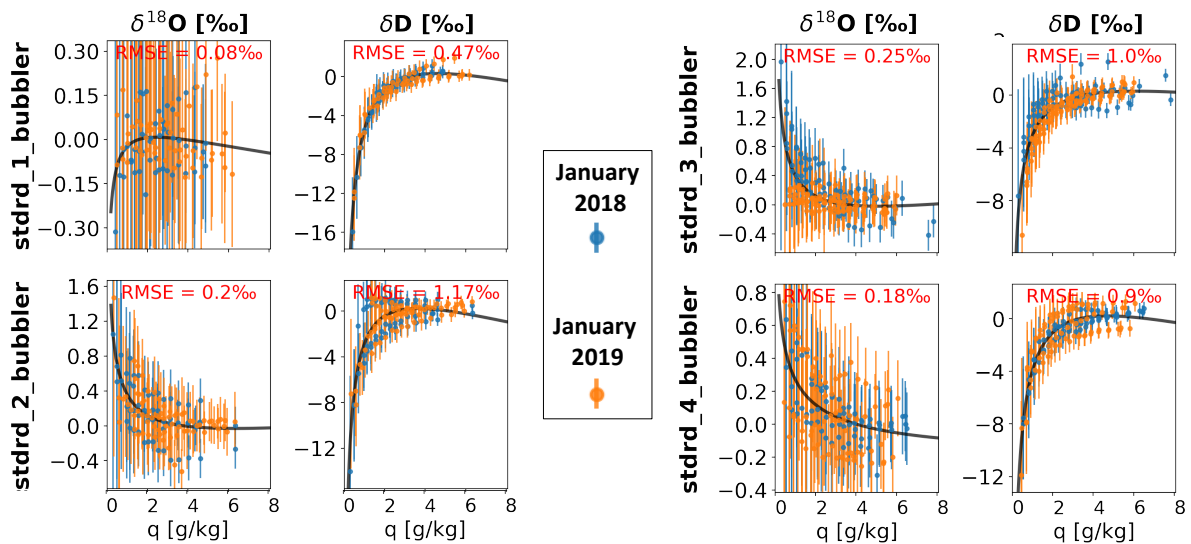


Figure 1. (Figure A1 in the revised manuscript). Humidity response function curves for different standards at different specific humidity levels for  $\delta^{18}O$  and  $\delta D$ . The isotope measurements and their uncertainties (light blue lines) are plotted as anomaly values, calculated in relation to the mean value of the isotopic composition for every bubbler. The values are fitted by a second degree polynomial curve (dark blue line).

*- It is not clear why the diurnal cycles are not shown in this study while they are expected to bring interesting information, especially when comparing to other sites as performed in sections 4.4.1 and 4.4.2. It is thus important that the diurnal cycles (at least in summer) are shown and thoroughly discussed. Otherwise, the comparison performed on section 4.4 on the correlation of the isotopic signal does not make sense since they are done on different timescales.*

We agree with this suggestion and have now additionally analysed the diurnal cycles, considering two months of two sequent summers (December-January of 2017/18 and 2018/19), in order to compare our data with previously reported studies of the diurnal cycle in Antarctica. We added the subsection “Diurnal cycle” to the paper (revised manuscript, Subsection 3.5). In the Discussion section, we discuss our new results:

Revised manuscript, Subsection 3.5, line 350:

### 3.5 Diurnal cycle

To evaluate the diurnal cycles at Neumayer Station, we consider two months of two sequent summers (December-January of 2017/18 and 2018/19) in order to compare our results with previous studies performed in Antarctica. We derive the daily mean values (the mean of 24 hourly mean values for each day) and subtract it from the time series. The remaining anomalies of all parameters represent an average diurnal cycle (Fig. 8).

The average of all values of each variable for the diurnal cycle study period (December-January of 2017/18 and 2018/19) are:  $\delta^{18}\text{O}$ : -26.34 ‰;  $\delta\text{D}$ : -205.27 ‰;  $d$ : 5.46 ‰; 2-meter temperature: -4.25 °C; 10-meter temperature: -3.87 °C; specific humidity: 2.49 g kg<sup>-1</sup>; relative humidity: 86.30 %; wind speed: 7.53 m s<sup>-1</sup>; wind direction: 291 degree (we consider only winds with a wind speed of more than 3 m s<sup>-1</sup>); shortwave downward radiation: 228.98 Wm<sup>-2</sup>.

Strong diurnal cycles in 2-meter temperature (Fig. 8d, red line), 10-meter temperature (Fig. 8d, green line), specific humidity (Fig. 8e), and relative humidity (Fig. 8f) are detected. For wind speed, the diurnal cycle is weak (Fig. 8g) and for wind direction no diurnal cycle is detectable (Fig. 8h). In summer, there is no strong temperature inversion close to the surface, at least not for the first 10 meters above surface. The temperature differences between 2-meter and 10-meter height reaches up to 1 °C during the coldest time of a day, while during half of the day their difference is less than 0.4 °C. The amplitudes of 10-meter temperature (3.63 °C) are less than 2-meter temperature (4.14 °C). The amplitudes of the specific humidity and relative humidity are 0.54 g kg<sup>-1</sup> and 4.19 %, respectively.

A clear diurnal cycle can be detected for  $\delta^{18}\text{O}$  (Fig. 8a),  $\delta\text{D}$  (Fig. 8b), and  $d$  (Fig. 8c). The diurnal amplitudes are 2.45 ‰, 21.07 ‰, and 4.87 ‰, respectively. A very high correlation coefficient between  $\delta^{18}\text{O}$  and 2-meter temperature ( $r = 0.98$ ) and 10-meter temperature ( $r = 0.99$ ) suggests the temperature changes as the main driver of water vapour  $\delta^{18}\text{O}$  diurnal variations.  $d$  is rather anti-correlated with relative humidity ( $r = -0.59$ ), while it does not show a considerable correlation with temperature and specific humidity.

The 2 and 10-meter temperature cycles and consequently  $\delta^{18}\text{O}$  and  $\delta\text{D}$  follow the shortwave radiation (Fig. 8i) with a short delay (around 3 hours) and show the minimum and maximum values at 03:00 UTC (local time) and 15:00 UTC. The relative humidity behaves the other way

round and shows the minimum value at 15:00 UTC and and maximum values between 21:00 UTC and 03:00 UTC.  $d$  has the minimum at 00:00 UTC and the maximum at 09:00 UTC.

Revised manuscript, Subsection 3.5, Figure 8:

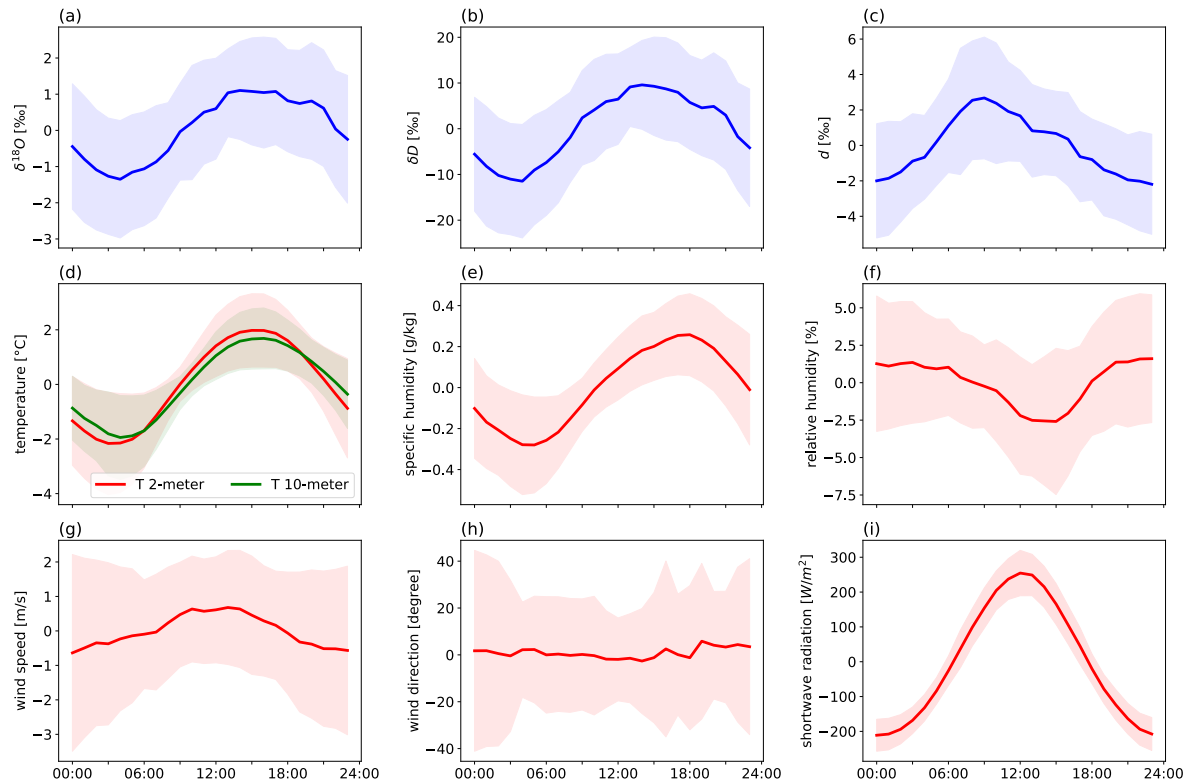


Figure 2 (Figure 8 in the revised manuscript). Anomaly diurnal cycles of (a)  $\delta^{18}\text{O}$  [‰], (b)  $\delta\text{D}$  [‰], (c)  $d$  [‰], (d) 2-meter temperature and 10-meter temperature [°C], (e) specific humidity [ $\text{g kg}^{-1}$ ], (f) relative humidity [%], (g) wind speed [ $\text{m s}^{-1}$ ], (h) wind direction [degree], (i) shortwave downward radiation [ $\text{W m}^{-2}$ ], and their  $\pm 1$  standard deviations for two months of two sequent summers (December-January of 2017/18 and 2018/19). Blue colour shows the Picarro instrument measurements and red colour (and green) shows meteorological observations at Neumayer Station. The local time zone at Neumayer Station is equal to UTC time.

Added to Discussion section:

Revised manuscript, Subsubsection 4.3.1, line 463:

To analyse changes during the diurnal cycle, Bréant et al. (2019) categorized their measurements based on the weather conditions as days with a clear sky and days with a cloudy sky. Since we do not find large differences in diurnal cycles related to these two conditions at Neumayer Station, we do not cluster our measurements. At both stations, strong diurnal cycles in  $\delta^{18}\text{O}$ ,  $\delta\text{D}$ ,  $d$ , temperature and specific humidity are observed. The diurnal cycle of the mostly katabatic winds is stronger at Dumont d’Urville station than Neumayer Station. At Dumont d’Urville station, a relatively low correlation between the diurnal cycle of temperature and  $\delta^{18}\text{O}$  shows that the temperature cannot be the main driver of  $\delta^{18}\text{O}$  variations, while at Neumayer Station it is the main driver of diurnal variations of  $\delta^{18}\text{O}$ . At Dumont d’Urville station, diurnal

cycle links start with the temperature variations in the continental areas above the station due to the incoming shortwave radiation diurnal cycle. A decrease of incoming shortwave radiation leads to radiative cooling at the continental slopes surface (above the station), resulting in an increase of the katabatic wind, which is characterized by lower  $\delta^{18}\text{O}$  and higher  $d$  values and thus causes the diurnal cycles at Dumont d'Urville station. At Neumayer Station, the shortwave radiation affects mainly the local temperature results in  $\delta^{18}\text{O}$  value variations, while the dominant wind, in the absence of the strong katabatic wind, is from east.

Added to Discussion section:

Revised manuscript, Subsubsection 4.3.2, line 500:

Ritter et al. (2016) chose 18 days of their available measurements to evaluate the diurnal cycles at Kohlen Station. They observed a strong diurnal cycle in temperature, specific humidity, wind speed (mostly katabatic),  $\delta^{18}\text{O}$ ,  $\delta\text{D}$  and  $d$ , while at Neumayer Station, a weak daily cycle of wind changes (mostly from east) is detected. For the diurnal variations at Kohlen Station, there exist high correlations between specific humidity and  $\delta\text{D}$  ( $r = 0.99$ ) and also between temperature and  $\delta\text{D}$  ( $r = 0.99$ ) which highlight the role of 495 temperature in  $\delta\text{D}$  and  $\delta^{18}\text{O}$  diurnal cycles. In contrast to Neumayer Station, the  $d$  values are strongly anti-correlated with  $\delta^{18}\text{O}$  and  $\delta\text{D}$  at Kohlen Station. Ritter et al. (2016) suggested that this strong anti-correlation is caused by a distillation effect at very low temperatures (mean temperature at Kohlen station during their campaign is  $-23.40\text{ }^\circ\text{C}$ ).

The information of the available summer data sets from these three locations (Neumayer Station, Dumont d'Urville, Kohlen Station) are summarized in Table 1.

*Table 1. (Table 1 in the revised manuscript). Comparison of summer water vapour isotope studies in different Antarctic stations (Ritter et al., 2016; Bréant et al., 2019). The time period of each study is shown in the table. For Neumayer Station, two months of two summers (December 2017/January 2018 and December 21018/January 2019) are considered.*

Diurnal cycle parameter	Neumayer	Dumont d'Urville	Kohlen
diurnal cycle period	all days	only clear sky periods	20/12/2013 - 27/12/2013
temperature [ $^\circ\text{C}$ ]	average value: -4.24 diurnal cycle amplitude: 4.14	average value: -0.5 diurnal cycle amplitude: 4.5	average value: -23.4 diurnal cycle amplitude: 8.7
specific humidity [ $\text{g kg}^{-1}$ ]	average value: 2.49 diurnal cycle amplitude: 0.54	average value: 1.99 diurnal cycle amplitude: 0.80	average value: 0.74 diurnal cycle amplitude: 0.62
wind [ $\text{m s}^{-1}$ ]	average value: 7.5 diurnal cycle amplitude: 1.5	average value: 8 diurnal cycle amplitude: 7	average value: 4.5 diurnal cycle amplitude: 3.5
$\delta^{18}\text{O}$ [‰]	average value: -26.34 diurnal cycle amplitude: 2.45	average value: -30.37 diurnal cycle amplitude: 5.40	average value: -54.74 diurnal cycle amplitude: 4.87
$d$ [‰]	average value: 5 diurnal cycle amplitude: 5	average value: 3 diurnal cycle amplitude: 10	average value: 30 diurnal cycle amplitude: 11

*- The slope of the relationship between  $q(\text{picarro})$  and  $q(\text{meteorology})$  is very high (1.5). This is really surprising. It would be better to have a direct calibration of the humidity of the picarro (in laboratory using a dew point generator for example).*

We have analysed the different  $q$  values now in more detail and expanded the corresponding text in the revised manuscript:

Revised manuscript, Subsection 3.1, line 193:

We compare the specific humidity measured by the Picarro instrument with the specific humidity values measured routinely as part of the meteorological observations at Neumayer Station (Schmithüsen et al., 2019). The relationship between these two series of humidity measurements is  $q(\text{Picarro}) = 1.5q(\text{meteorology}) + 0.08$  ( $N = 12198$ , hourly values between 17 February 2017 and 22 January 2019,  $r = 0.97$ , standard error of the estimate =  $0.0022 \text{ g.kg}^{-1}$ ; revised manuscript, Fig. 3). The rather high slope between both humidity measurements and also a number of unusual high and low Picarro humidity values motivated us to analyse the difference between both humidity data sets in more detail.

The inlet of the Picarro instrument is situated approx. 17.5 m above the surface level of the station. As the station is placed on a small artificial hill, this surface level is approx. 7.6 m higher than the surface level of the meteorological mast placed 50 meters besides the station building. Thus, the total height difference between the Picarro inlet and the height of the meteorological humidity measurements is approx. 22 m. In principle, higher humidity values at the Picarro inlet could be explained by a humidity inversion layer above the surface, which could remove near-surface moisture at the meteorological mast position by hoar frost formation. However, temperature differences between a 2-meter temperature sensor at the meteorological mast and temperatures measured on the roof of the station do not exceed  $2 \text{ }^\circ\text{C}$  during our measurement period. No strong temperature inversions are found for the days with extreme Picarro humidity measurements.

To test if contamination by exhaust gases could be another reason for the data mismatch, the wind direction was analysed for those hourly Picarro humidity values which are much higher than the corresponding humidity values measured by the meteorological station. Most of the outliers coincide with a wind direction from the south (and a few from east), which excludes the possibility that a contamination by exhaust gases is the reason for the unusually high Picarro humidity values.

Picarro humidity measurements have been compared with independent humidity observations for a few studies, so far. Aemisegger et al. (2012) calibrated and controlled the humidity of their Picarro instrument by a dew point generator and showed a linear relationship between Picarro measurements and the humidity measured by the calibration system with a slope of 1.27 and an uncertainty of 100-400 ppm ( $0.06\text{-}0.24 \text{ g.kg}^{-1}$ ). Tremoy et al. (2011) reported that the slope between humidity measured by a meteorological sensor and humidity measured by a Picarro instrument can change from 0.81 to 1.47 depending on site conditions. Bonne et al. (2014) also showed a non-linear response of their Picarro instrument compared with the humidity measured by a meteorological sensor. Based on their data, the ratio between Picarro humidity and sensor humidity values changed from 1 to 1.87, depending on the amount of

humidity. Compared to the results of these studies, we rate the calculated ratio of our Picarro humidity measurements versus the humidity data from the meteorological mast ( $q_{\text{Picarro}}/q_{\text{meteorology}} = 1.5$ ) as unobstructive.

As in previous studies (e.g., Bonne et al., 2014) we will use the Picarro humidity data for the calculation of the humidity response functions required for the calibration of the isotope measurements. All analyses regarding the relationships between water vapour isotopes and local climate variables, on the other hand, are based on the humidity and corresponding temperature data measured at the meteorological mast.

*- Some d-excess peaks look strange and are not discussed (e.g. negative peak in August or September 2018). Also the authors should explain why some periods are lacking in the record.*

We looked at the data with one hour resolution and did not find any unusual explanation for these peaks. In a follow-up study, we will look at the data with high temporal resolution, then we can focus more on these special periods. The missing periods are explained in the text:

Revised manuscript, Subsection 3.1, line 189:

“There exist some data gaps for isotope values for these two years of measurements. Water vapour isotope data is missing at some days because of maintenance or reparation of the instrument, measuring humidity response functions, or due to the removal of data outliers related to instable measurements of the Picarro instrument. In total, daily vapour and isotope data exists for 600 out of 705 days (85 %).”

*- I do not see the interest of looking at the d18O vs temperature, then d18O vs ln(q) and then temperature vs ln(q). . . . The link between temperature and ln(q) can be mentioned in one sentence early in the manuscript stating that the Clausius-Clapeyron relationship is dominating the humidity signal at Neumayer and then remove Figure 5 and Figure 9.*

We agree with this suggestion and have removed Fig. 5 and Fig. 9 from the manuscript. The link between specific humidity and atmospheric temperature through Clausius–Clapeyron relation is explained with a proper citation:

Revised manuscript, Subsubsection 3.2.1, line 286:

At Neumayer Station, the specific humidity is highly correlated with temperature (Jakobs et al., 2019), as expected from the general Clausius-Clapeyron relation between both quantities. As a consequence, the  $\delta^{18}\text{O}$  values of water vapour at Neumayer Station are strongly correlated not only to temperature, but also to specific humidity ( $r = 0.85$ ).

*- The appendix with the d-excess correlations is not useful – you could simply detail what is statistically robust or not in the correlation in section 3.2.3.*

Corrected as suggested:

revised manuscript, Subsubsection 3.2.2 line 296:

For the Deuterium excess, an overall weak negative correlation between  $\delta^{18}\text{O}$  and  $d$  ( $r = -0.35$ ) is found. The anti-correlation between  $\delta\text{D}$  and  $d$  is weaker ( $r = -0.24$ ). For  $d$ , the correlation with 2 m temperature is low and negative ( $r = -0.33$ ). The corresponding correlation of the specific humidity with  $d$  is stronger ( $r = -0.48$ ).

Analysing different seasons of the year, a negative correlation between  $\delta^{18}\text{O}$  and  $d$  is detected for spring,  $r = -0.47$ , summer,  $r = -0.51$ , and autumn,  $r = -0.37$ , but for winter, no correlation exists. This pattern can be detected also for temperature- $d$ , specific humidity- $d$ , and relative humidity- $d$  relations. There is a negative correlation coefficient between temperature and  $d$  for spring,  $r = -0.41$ , summer,  $r = -0.60$ , and autumn,  $r = -0.14$ , but in winter a weak positive correlation,  $r = 0.22$ , is noticed. There are anti-correlations between the specific humidity (relative humidity) values and  $d$  for spring,  $r = -0.50$  ( $r = -0.43$ ), summer,  $r = -0.71$  ( $r = -0.59$ ), and autumn,  $r = -0.24$  ( $r = -0.19$ ), which are slightly stronger than the ones between temperature and  $d$ . For winter, there is a weak positive correlation between the specific humidity and  $d$ ,  $r = 0.13$ , ( $r = 0.04$ ).

*- I do not understand the sentence on l. 285 -> do you have any measurements (isotopes, temperature, humidity . . .) over some characteristic events showing that  $d18\text{O}$  values drop intensively in a distance of 16 km between open sea and the station? If not, such affirmation should be removed.*

We do not have any measurements. It is removed as suggested.

*- I am not sure that the Figure 11 corresponds very well to the text. The association between wind from the East and higher  $d18\text{O}$  only works for 22 out of 36 days (61% - not sure to understand where does the 64% value comes from) which is not a proportion strong enough to drive such conclusion on Figure 11. The signal is increased when considering only extremely warm and cold days.*

The figure is a summary for common windy situations at Neumayer Station. But the sentence “Wind patterns and their effect are summarized in Fig. 11” may have been misplaced. The text is now reformulated and contains some additional explanations. In the revised manuscript, first,

we analyse days with temperature events. The sentence “General wind patterns and their effects at Neumayer Station are sketched in Fig. 10.” is placed at the end of the paragraph:

Revised manuscript, Subsubsection 4.1.2, line 386:

Next, we analyse the impact of another meteorological factor, wind, on the isotope values in vapour at Neumayer Station. During the observation period, on 86 % of all days that involve warm events at Neumayer Station, the wind came from east. Such wind conditions are usually a result of a low-pressure system north of the station (König-Langlo et al., 1998; König-Langlo, 2017). In such a situation, the weather at Neumayer Station is typically relatively warm with high relative humidity (88% of days with a relative humidity higher than 90% coincide with wind from east) and cloudiness (85% all cloudy days, i.e. days with a total cloud amount of more than 80%, coincide with this wind direction). Relatively higher temperature and specific humidity lead to more enriched  $\delta^{18}\text{O}$  values. During days that involve cold events, the winds typically come from south to south-west and wind speeds are rather low. This weather pattern occurs when a cyclone has moved eastward, so that the former low-pressure area is replaced by a high-pressure ridge. In such a situation, wind speeds decrease and the wind direction changes from easterly to southerly and south-westerly. The weak katabatic winds are strengthened by the synoptically caused air flow and bring cold and dry air from East Antarctic Plateau to Neumayer Station, usually dissolving the clouds. Lower temperature and specific humidity result in more depleted  $\delta^{18}\text{O}$  in water vapour coming to Neumayer Station. General wind patterns and their effects at Neumayer Station are sketched in Fig. 10.

*- It is not clear which types of events the authors want to discuss in section 4.2 for the key controls on vapour  $d$ -excess. Indeed, synoptic events lasting several days and associated with a particular atmospheric pattern will not necessarily be detected by the proposed algorithm: if several following days have a particularly high  $d$ -excess values then the average value over 10 days may also be high and the period will not be identified. Moreover, the  $d$ -excess pattern found with this definition are not very clear and no clear explanation of the pattern is provided (observed correspondence apply to 70% or less of observed cases). This section is thus not very strong.*

We have changed the number of days from 10 days to 15 days. This action allowed us to discover more days as high or low  $d$  days. We also agree that the comparison of high or low  $d$  values with average values of temperature and humidity was not sound enough. Thus, we removed this part and focus now on days with high and low  $d$  values, considering the origin of the water vapour and moisture uptake places:

Revised manuscript, Subsection 4.2, line 414:

Changes of  $d$  in vapour generally are supposed to reflect different climate conditions at the moisture source region (Merlivat and Jouzel, 1979; Pfahl and Sodemann, 2014) and recognized

as a tracer that point out the origin of the water vapour (Gat, 1996). Other, less dominant factors that effect  $d$  are the amount of condensation from source to sink, which is ruled out here since there is no systematic anti-correlation between  $d$  and  $\delta D$ .

In order to better understand the effect of different pathways and water moisture origins that control  $d$  changes in vapour at the station, days with extreme values of  $d$  are examined. As no long-term measurements for  $d$  in water vapour at Neumayer Station exist, we cannot define extreme  $d$  values considering multi-year daily average (as done for the analysis of extreme temperature events). Thus, we define extreme  $d$  values as daily averaged  $d$  values which are one standard deviation higher or lower than the 14-days average value centered around the corresponding day (7 days before and 7 days after). Analysing the simulated moisture uptake for days with low and high  $d$  values reveals the influence of the origin of the water vapour on extreme  $d$  values (revised manuscript, Fig. 11). The moisture corresponding to low daily  $d$  values is either uptaken in coastal areas east of the station (this occurs mostly in summer) or north-west of it in the South Atlantic Ocean. For such low  $d$  values of a marine moisture origin, sea surface temperature and near-surface relative humidity are the prime controls (Merlivat and Jouzel, 1979). The occurrence of high  $d$  in water vapour originating from a sea surface area close to a sea ice margin has been explained by different studies such as Kurita (2011) and Steen-Larsen et al. (2013). Based on the back trajectory simulations, the high  $d$  values in our measurements can be explained in a similar way. Strong evaporation from sea surface waters into cold humidity-depleted polar air close to the ice-margin (here, areas close to Neumayer Station) will result in strong kinetic effects providing higher  $d$  values in the water vapour.

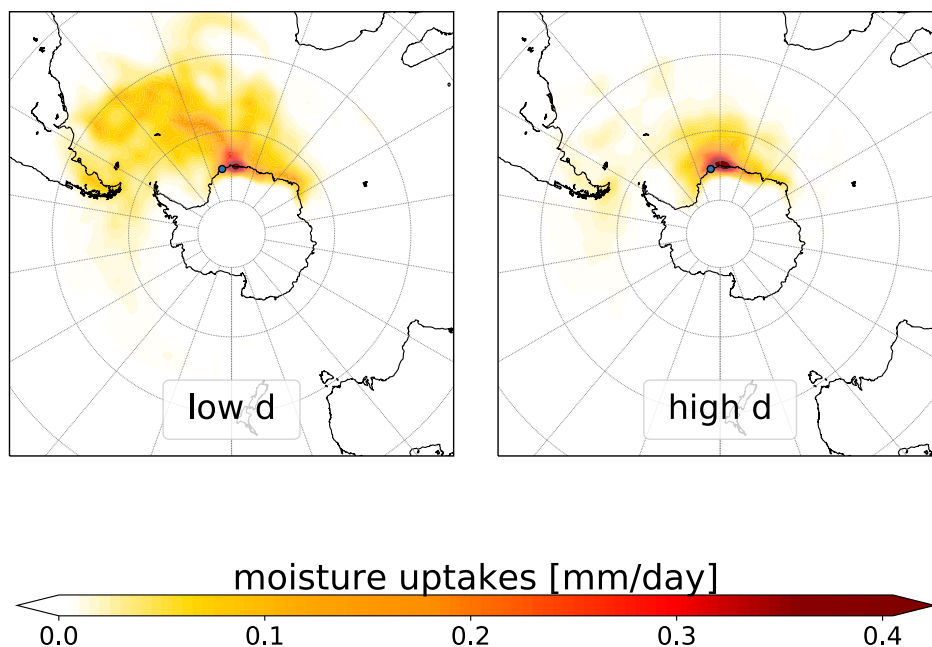


Figure 3. (Figure 11 in the revised manuscript). Simulated moisture uptake occurring within the boundary layer [ $\text{mm day}^{-1}$ ] towards Neumayer Station modelled by FLEXPART for the whole period of the experiment, left: an average on days with low  $d$  events, right: an average on days with high  $d$  events.

*- The section 4.3 should be placed earlier (not in the discussion section)*

Corrected as suggested.

Revised manuscript, Subsection 3.4, line 334:

Wind direction and wind speed are two of the main factors used in our back trajectory calculations to determine the origin of air parcels heading to Neumayer Station. To check the robustness of our results, we compare ERA5 data wind data, which is used in this study for FLEXPART simulations to identify moisture sources and transport pathways to Neumayer Station, with meteorological observations from Neumayer Station. The comparison reveals that the ERA5 dataset reproduces wind direction and wind speed around Neumayer Station well for most days (revised manuscript, Fig.6). However, for cold events, the ERA5 dataset has a bias with respect to the katabatic winds (revised manuscript, Fig. 6c), although the Neumayer Station meteorological data is assimilated in ERA5. The main reason for this bias in the ERA5 data might be the low number of stations in Antarctica, which are used to generate the ERA5 reanalysis dataset. Due to this bias in the ERA5 data, the simulated moisture uptake and vapour transport pathways during cold events, when katabatic winds from the south and south-west occur at Neumayer Station, should be taken with caution.

*- Section 4.4 cannot stand like this without showing also daily variability at Neumayer*

As mentioned above, the “Diurnal cycle” subsection is added to the paper (revised manuscript, Subsection 3.5) and discussed in the “Discussion” section.

*- The section 4.5 aims at discussing the air-snow interaction but the fresh snow is sampled only after major snowfall events which is very different to the other study discussed here (Steen-Larsen et al., 2014) in which snow was sampled at high resolution in presence or absence of precipitation. It is thus impossible to discuss the link between air and snow in the case presented here when surface snow is only sampled after large snowfall events. In this case surface snow isotopic composition reflects the isotopic composition of the precipitation.*

We fully agree with the referee’s comment on difference of the cited studies. Therefore, we reformulated the text section and explain our results and its difference to other studies in more details:

Revised manuscript, Subsection 4.4, lines 531:

Recently, several studies have reported an exchange of water isotopes between surface snow and the vapour above the surface for Greenland (Steen-Larsen et al., 2014a; Madsen et al.,

2019) and Antarctica (Casado et al., 2018). Steen-Larsen et al. (2014a) showed in their case study in Greenland, that surface snow  $\delta^{18}O$  between snowfalls events, follows  $\delta^{18}O$  in water vapour with similar or smaller changes than the water vapour  $\delta^{18}O$ . The authors suspect that surface snow isotopes are driven by changes in the water vapour isotopic compositions. In our study, the agreement in the T- $\delta^{18}O$  slopes and also in the  $\delta^{18}O$ - $\delta D$  slopes for water vapour and snow samples measured at Neumayer Station is remarkable. Thus, the isotopic exchange between water vapour and surface snow at this location should be further examined in more detail in future research studies. Since our study provided water vapour isotopic composition measurements with a high temporal resolution and the water vapour isotope monitoring is continuously running at Neumayer Station, we plan to compare the isotope data of water vapour and snow in more detail in the future. If surface snow isotopic compositions are derived by changes in water vapour isotopes, ice core water isotope records might be interpreted as continuously recorded paleoclimate signals, even for periods without any precipitation.

*Summarizing, the whole discussion section is rather weak and additional work should be done on it to make a better use of the new data set.*

We see the uniqueness of this manuscript in the initial presentation of this new Antarctic water vapour isotope data set. We agree with the referee that some of our first analyses of the data set are rather basic, and that additional work could be done for further exploiting the data. Following his/her suggestions, we have added a new analysis of the diurnal cycle of water isotopes at Neumayer to this study (Subsection 3.5). We also extended our FLEXPART analyses of moisture sources and transport pathways to the full 2-year observation period. Further in-depth analyses of the data set will follow in future studies.

Overall, we have substantially improved the manuscript based on the specific comments of this referee and of two other anonymous referees. We hope that we have dealt with all comments in an adequate manner and that the revised manuscript now qualifies for publication in The Cryosphere.

## References

- Aemisegger, F., Sturm, P., Graf, P., Sodemann, H., Pfahl, S., Knohl, A., and Wernli, H.: Measuring variations of  $\delta^{18}\text{O}$  and  $\delta^2\text{H}$  in atmospheric water vapour using two commercial laser-based spectrometers: an instrument characterisation study, *Atmos. Meas. Tech.*, 5, 1491–1511, <https://doi.org/10.5194/amt-5-1491-2012>, 2012.
- Bonne, J.-L., Masson-Delmotte, V., Cattani, O., Delmotte, M., Risi, C., Sodemann, H., and Steen-Larsen, H. C.: The isotopic composition of water vapour and precipitation in Ivittuut, southern Greenland, *Atmos. Chem. Phys.*, 14, 4419–4439, <https://doi.org/10.5194/acp-14-615-2014>, 2014.
- Bréant, C., Dos Santos, C. L., Agosta, C., Casado, M., Fourré, E., Goursaud, S., Masson-Delmotte, V., Favier, V., Cattani, O., Prié, F., et al.: Coastal water vapor isotopic composition driven by katabatic wind variability in summer at Dumont d’Urville, coastal East Antarctica, *Earth Planet. Sc. Lett.*, 514, 37–47, <https://doi.org/10.1016/j.epsl.2019.03.004>, 2019.
- Casado, M., Landais, A., Picard, G., Münch, T., Laepple, T., Stenni, B., Dreossi, G., Ekaykin, A., Arnaud, L., Genthon, C., Touzeau, A., Masson-Delmotte, V., and Jouzel, J.: Archival processes of the water stable isotope signal in East Antarctic ice cores, *The Cryosphere*, 12, 1745–1766, <https://doi.org/10.5194/tc-12-1745-2018>, 2018.
- Gat, J. R.: OXYGEN AND HYDROGEN ISOTOPES IN THE HYDROLOGIC CYCLE, *Annu. Rev. Earth Pl. Sc.*, 24, 225–262, <https://doi.org/10.1146/annurev.earth.24.1.225>, 1996.
- Jakobs, C. L., Reijmer, C. H., Kuipers Munneke, P., König-Langlo, G., and van den Broeke, M. R.: Quantifying the snowmelt–albedo feedback at Neumayer Station, East Antarctica, *The Cryosphere*, 13, 1473–1485, <https://doi.org/10.5194/tc-13-1473-2019>, 2019.
- König-Langlo, G.: Basic and other measurements, and meteorological synoptical observations from Neumayer Station, 1992-04 to 2016-01, reference list of 572 datasets, <https://doi.org/10.1594/PANGAEA.874984>, 2017.
- König-Langlo, G., King, J., and Pettré, P.: Climatology of the three coastal Antarctic stations Dumont d’Urville, Neumayer, and Halley, *J. Geophys. Res. Atmos.*, 103, 10 935–10 946, <https://doi.org/10.1029/97JD00527>, 1998.
- Kurita, N.: Origin of Arctic water vapor during the ice-growth season, *Geophys. Res. Lett.*, 38, <https://doi.org/10.1029/2010GL046064>, 2011.
- Madsen, M. V., Steen-Larsen, H. C., Hörhold, M., Box, J., Berben, S. M. P., Capron, E., Faber, A.-K., Hubbard, A., Jensen, M. F., Jones, T. R., Kipfstuhl, S., Koldtoft, I., Pillar, H. R., Vaughn, B. H., Vladimirova, D., and Dahl-Jensen, D.: Evidence of Isotopic Fractionation During Vapor Exchange Between the Atmosphere and the Snow Surface in Greenland, *J. Geophys. Res. Atmos.*, 124, 2932–2945, <https://doi.org/10.1029/2018JD029619>, 2019.
- Merlivat, L. and Jouzel, J.: Global climatic interpretation of the deuterium-oxygen 18 relationship for precipitation, *J. Geophys. Res. Oceans*, 84, 5029–5033, <https://doi.org/10.1029/JC084iC08p05029>, 1979.
- Pfahl, S. and Sodemann, H.: What controls deuterium excess in global precipitation?, *Clim. Past*, 10, 771–781, <https://doi.org/10.5194/cp-10-771-2014>, 2014.
- Ritter, F., Steen-Larsen, H. C., Werner, M., Masson-Delmotte, V., Orsi, A., Behrens, M., Birnbaum, G., Freitag, J., Risi, C., and Kipfstuhl, S.: Isotopic exchange on the diurnal scale between near-surface snow and lower atmospheric water vapor at Kohnen station, East Antarctica, *The Cryosphere*, 10, 1647–1663, <https://doi.org/10.5194/tc-10-1647-2016>, 2016.

Schmithüsen, H., König-Langlo, G., Müller, H., and Schulz, H.: Continuous meteorological observations at Neumayer Station (2010-2018), reference list of 108 datasets, <https://doi.org/10.1594/PANGAEA.908826>, 2019.

Steen-Larsen, H. C., Johnsen, S. J., Masson-Delmotte, V., Stenni, B., Risi, C., Sodemann, H., Balslev-Clausen, D., Blunier, T., Dahl-Jensen, D., Ellehøj, M. D., Falourd, S., Grindsted, A., Gkinis, V., Jouzel, J., Popp, T., Sheldon, S., Simonsen, S. B., Sjolte, J., Steffensen, J. P., Sperlich, P., Sveinbjörnsdóttir, A. E., Vinther, B. M., and White, J. W. C.: Continuous monitoring of summer surface water vapor isotopic composition above the Greenland Ice Sheet, *Atmos. Chem. Phys.*, 13, 4815–4828, <https://doi.org/10.5194/acp-13-4815-2013>, 2013.

Tremoy, G., Vimeux, F., Cattani, O., Mayaki, S., Souley, I., and Favreau, G.: Measurements of water vapor isotope ratios with wavelength-scanned cavity ring-down spectroscopy technology: new insights and important caveats for deuterium excess measurements in tropical areas in comparison with isotope-ratio mass spectrometry, *Rapid Commun. Mass Sp.*, 25, 3469–3480, <https://doi.org/https://doi.org/10.1002/rcm.5252>, 2011.